Solar Energy, Vol. 13, pp. 43–57. Pergamon Press, 1970. Printed in Great Britain

THE MEASUREMENT OF SOLAR SPECTRAL IRRADIANCE AT DIFFERENT TERRESTRIAL ELEVATIONS*

E. G. LAUE†

(*Received* 26 *June* 1969)

Abstract—The increasing world population and the increasing complexity of civilization require improved efficiency in the utilization of natural resources. Solar energy is the primary determinate of our environment, and an understanding of the nature of its irradiance is fundamental in the control or modification of human and biological ecology. Recent improvements in filter radiometry have resulted in the realization of simple robust instruments facilitating spectral irradiance determinations, in wavelength bands as narrow as 100 nm, throughout the solar spectrum. Application of these instruments, utilizing jet rocket aircraft, has extended our knowledge of the solar spectral irradiance at altitudes up to 80 km. This paper indicates the methods necessary to obtain such spectral data and presents some ground-based summaries and, in particular, new results of concurrent measurements made at 1·3 and 2·3 km; the meteorological interpretation is indicated. Since knowledge of the variation of such radiant energy fluxes at various locations on the Earth's surface is meagre, it is difficult to assess the potential application. Initial efforts might entail, as a minimum requirement, a three-channel bandpass system monitoring the total, ultraviolet and infrared irradiances. Data from this system could provide useful information concerning the local aerological situation. The need for extension of investigations in this field is urgent.

Résumé—La croissance de la population mondiale et la complexité grandissante de notre civilisation demandent une meilleure utilisation des ressources naturelles. L'énergie solaire est le premier facteur déterminant de notre milieu et comprendre la nature de son rayonnement est fondamental pour contrôler ou modifier l'écologie humaine et biologique. Les perfectionnements récents effectués dans le domaine de la radiométrie des filtres ont abouti à la réalisation d'instruments simples et robustes permettant de déterminer plus facilement le rayonnement spectral, dans des bandes de longueurs d'ondes aussi étroites que 100 nm, pour tout le spectre solaire. L'application de ces instruments, par avion-fusée, a étendu nos connaissances du rayonnement du spectre solaire à des altitudes allant jusqu'à 80 km. Cet article présente les méthod pour obtenir de telles données spectrales et présente quelques résumés au sol et, en particulier, de nouveaux résultats de mesures concurrentes effectuées a 1,3 et 2,3 km. On donne l'interprétation météorologique. Les connaissances de la variation de tels flux d'énergie radiante en divers endroits de la surface de la terre sont si maigres qu'il est difficile d'évaluer le potentiel d'application. Des efforts préliminaires peuvent donner suite, tout au moins pour le minimum, à un système de passage de bande à trois voies contrôlant la totalité des rayonnements de l'ultraviolet et de l'infrarouge. Les données de ce système pourraient fournir des informations utiles concernant la situation locale aérologique. Il existe un besoin urgent d'étendre les recherches dans ce domaine.

Resumen—Ante el constante aumento de la población mundial y la creciente complejidad de nuestra civilización, se hace necesario un aprovechamiento más efficaz de los recursos naturales. Siendo la energía solar el determinante primordial de nuestro medio ambiente, el conocer la naturaleza de su irradiación tiene carácter fundamental para poder controlar o modificar la ecología humana y biológica. Recientes perfeccionamientos en la radiometría por filtros han permitido la realización de instrumentos sencillos y robustos que simplifican las determinaciones de la irradiación espectral, en bandas de onda hasta de sólo 100 nm, a través de todo el espectro solar. La aplicación de tales instrumentos, con ayuda de aviones de reacción, ha extendido nuestro conocimiento de la irradiación del espectro solar en distintas altitudes hasta 80 km. Esta ponencia, tras indicar los métodos necesarios para conseguir tal información espectral, presenta algunos resúmenes con base en tierra, en particular los resultados conseguidos últimamente por medición concomitante a 1,3 y 2,3 km, exponiéndose la interpretación meteorológica de los mismos. Ante los pocos datos existentes sobre la variación de estos flujos de energía radiante en distintos puntos de la superficie terrestre, resulta difícil evaluar la aplicación potencial. Para una solución inicial es posible se necesite, como mínimo, un sistema de paso de banda con tres canales, que permita comprobar la irradiación total, ultravioleta e infrarroja. Los datos obtenidos mediante este sistema podrían contener información interesante acerca de la situación aerológica local. Urge ampliar las investigaciones en este terreno.

---

*This paper presents the results of one phase of research carried out at the Jet Propulsion Laboratory, California Institute of Technology, under Contract No. NAS 7-100, sponsored by the National Aeronautics and Space Adminstration. It is based on a 1968 Solar Energy Society Conference paper.

†Technical Staff: Jet Propulsion Laboratory, California Institute of Technology, Pasadena, Calif. 91103, U.S.A.

INTRODUCTION

MAXIMUM efficiency in the utilization of our natural resources is a prime necessity in our increasingly complex civilization. Weather and climate have a profound effect upon operations in the fields of manufacturing, agriculture, mining, construction and transportation industries. In the Los Angeles basin, at the present time, a significant portion of industry is affected by air pollution predictions. A smog forecast can cause manufacturers to shift their fuel consumption or postpone certain types of furnace operations. In the construction field, both long-range and short-range weather forecasts are utilized to schedule activities. The application of such advance weather information is obvious. The economic importance of correct frost warnings can involve literally millions of dollars and, more important, the saving of irreplaceable food. A significant reduction in storm and flood damage can be accomplished by more accurate and timely weather predictions. Since the solar energy absorbed by the terrestrial atmosphere provides the essential driving force for many weather phenomena, precise knowledge of this local absorption as well as its more general variation with altitude should provide a meaningful input to current meteorological computer programs. In the field of agriculture, it appears possible that the flowering and ripening of commercial crops could be better predicted if more specific information was available concerning the spectral distribution of solar irradiation in addition to the integral wavelength flux.

As demonstrated by Kunkel *et al.*[1], the spectral distribution of solar energy is critical in order to interpret the results of solar degradation tests. Terrestrial applications of solar energy can be improved if the spectral composition of the energy is better defined. The testing of solar panels, as power supplies for artificial satellites and spacecraft, is another activity wherein complete knowledge of the solar irradiance is necessary for proper interpretation of the test results.

Total solar irradiance measurements are now routinely made at many locations throughout the world, but solar spectral irradiance measurements have received less attention, principally because of the necessary complexity of the measurement systems. Figure 1 shows the classical series of solar spectral irradiance vs. optical air-mass curves prepared by Moon[2]; in 1940, this work represented the first efforts in this field. It must be emphasized that these curves are very generalized. However, the major modifiers of the atmospheric transmission, viz. Rayleigh and Mie scattering and water vapor and ozone absorption, are not necessarily the sole function of the relative air mass, defined as the secant of the Sun's zenith angle. A more recent attempt (see Tables 1 and 2) by Lopukhin[3] represents a method of classification where local solar spectral irradiance is related to moisture and aerosol contents. This work may point the way to a more adequate approach to classifying the spectral irradiance or, even better, to determining the atmospheric conditions above a site equipped to monitor the spectral irradiance. The recent work of Nader[4] concerning the ultraviolet irradiance and ultraviolet albedo measurements, as correlated to the Los Angeles basin smog conditions, represents a practical application of measurements of this kind to local meteorological conditions.

Hopefully, the techniques described here will be useful for investigations concerning the variance of the solar spectral irradiance, as related to the Earth's ecological relationships, and to encourage further efforts to introduce current technological capability into field applications.

Spectral information can be obtained through the use of two fundamental methods,

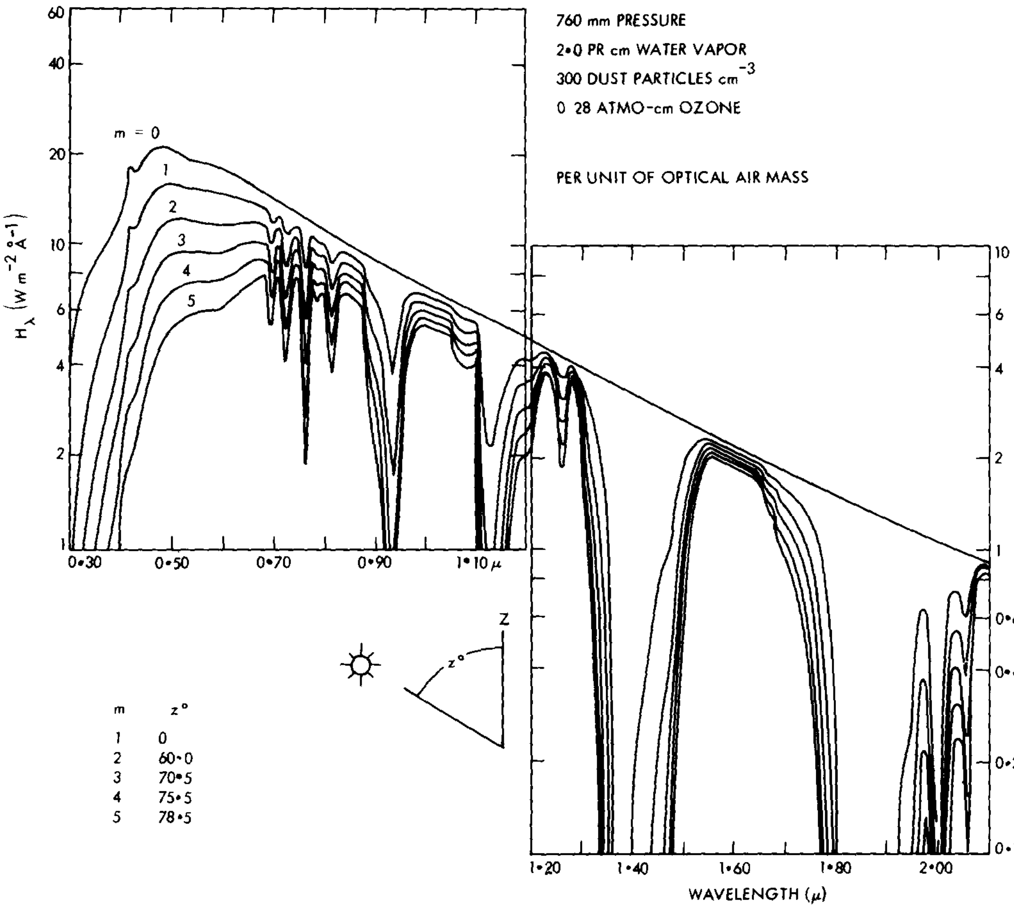

Fig. 1. Solar spectral irradiance curves at sea level for various optical air masses [2].

i.e. filter radiometry and monochromator spectroradiometry. The latter, by dispersion (with optical prisms or gratings) and then wavelength scanning of the spectrally dispersed energy, is the more elegant approach. A spectroradiometric system, such as that described by Arvesen [5], is capable of providing extremely detailed results concerning the spectral structure. Data acquired under conditions in which the total irradiance is highly constant over the instrument scan period (e.g. 30 min) can be integrated over any desired bandwidth with satisfactory accuracy. However, the size and cost of the equipment, the time required for a complete operation, and the need for computerizing the data limit this approach to major installations. In spite of modern automated techniques, it has been found that a skilled and experienced operator is generally required to produce valid spectral values.

Broad- and narrow-bandpass filter radiometric systems are much less complicated, more compact, and inherently more sturdy than dispersion-type instruments. On the other hand, wavelength resolution of filter techniques is limited by the energy available and the pass bands of the filters. Rapidity of data acquisition, which may be as short as 1–2 sec per channel, is limited only by the response time of the detector system.

Table 1. Spectral composition of direct solar radiation in lowland areas for different humidities and aerosols (after Lopukhin, 1957)

$\lambda_\odot$	Type I					Type II					Type III				
	S (cal/cm²/min)	% of total radiation for λ (nm)				S (cal/cm²/min)	% of total radiation for λ (nm)				S (cal/cm²/min)	% of total radiation for λ (nm)			
		290–380	290–520	520–606	>606		290–380	290–520	520–606	>606		290–380	290–520	520–606	>606
2	0·162	0·10	5·9	10·5	83·6	0·104	0·83	3·7	11·3	85·0	0·100	0·37	5·9	11·8	82·3
5	0·304	0·20	7·2	10·7	82·1	0·384	1·00	5·6	11·6	82·8	0·316	0·48	7·0	12·1	81·9
10	0·732	0·61	8·9	11·3	79·8	0·695	1·23	8·2	12·1	79·7	0·571	0·69	8·6	12·6	78·8
15	0·857	1·00	10·5	11·8	77·7	0·801	1·45	10·0	12·7	77·3	0·763	0·90	10·0	13·0	75·0
20	1·000	1·33	11·9	12·4	75·7	0·967	1·68	11·2	13·2	75·6	0·905	1·15	11·4	13·4	74·2
25	1·095	1·57	13·1	13·1	73·8	1·079	1·89	12·4	13·4	74·2	1·000	1·41	12·6	13·8	73·6
30	1·163	1·78	14·3	13·6	72·1	1·187	2·04	13·4	13·8	72·8	1·091	1·68	13·8	14·1	72·1
35	1·222	1·95	15·1	14·1	70·8	1·240	2·20	14·1	14·1	71·8	1·155	1·91	14·6	14·3	71·1
40	1·272	2·10	15·6	14·4	70·0	1·274	2·33	14·6	14·4	71·0	1·206	2·12	15·2	14·5	70·3
45	1·313	2·25	16·0	14·7	69·3	1·308	2·46	15·2	14·5	70·3	1·243	2·30	15·8	14·6	69·6
50	1·351	2·37	16·3	15·0	68·7	1·338	2·58	15·6	14·6	69·8	1·278	2·45	16·1	14·7	69·2
55	1·374	2·50	16·6	15·1	68·3	1·358	2·70	16·0	14·7	69·3	1·299	2·70	16·5	14·8	68·7
60	1·392	2·61	16·9	15·2	67·9	1·376	2·81	16·3	14·8	68·9	1·322	2·72	16·8	14·8	68·4
65	1·406	2·70	17·2	15·3	67·5	1·385	2·91	16·5	14·9	68·6	1·335	2·83	17·0	14·9	68·1
70	1·417	2·80	17·3	15·4	67·3	1·397	3·00	16·8	15·0	68·2	1·346	2·93	17·2	15·0	67·8
	$n = 27$;	$\alpha = 0{\cdot}67$;		$l = 6{\cdot}0$ mb		$n = 25$;	$\alpha = 0{\cdot}77$;		$l = 11{\cdot}7$ mb		$n = 32$;	$\alpha = 1{\cdot}16$;		$l = 8{\cdot}6$ mb	

Table 1. (*contd.*)

λ	Type IV					Type V					Type VI				
	S (cal/cm²/min)	% of total radiation for λ (nm)				S (cal/cm²/min)	% of total radiation for λ (m				S (cal/cm²/min)	% of total radiation for λ (nm)			
		290–380	290–520	520–606	>606		290–380	290–520	520–606	>606		290–380	290–520	520–606	>606
2	0·026	0·51	6·1	12·9	81·0	0·033	0·84	5·5	13·2	81·3	–	0·20	1·6	12·8	–
5	0·162	0·61	7·0	13·7	79·3	0·217	0·99	6·8	13·2	80·0	0·185	0·31	3·4	13·1	83·5
10	0·407	0·82	8·5	14·8	76·7	0·476	1·27	8·9	13·3	77·8	0·438	0·57	6·9	13·4	79·7
15	0·645	1·06	10·0	15·8	74·2	0·682	1·58	10·6	13·4	76·0	0·580	0·84	8·0	13·8	78·2
20	0·794	1·31	11·8	16·4	71·2	0·824	1·81	12·0	13·5	74·5	0·768	1·08	10·0	14·0	76·0
25	0·913	1·53	13·1	16·8	70·1	0·927	2·01	13·2	13·5	73·3	0·877	1·32	11·7	14·2	74·1
30	0·995	1·72	14·0	17·0	69·0	1·022	2·19	14·4	13·6	72·0	0·962	1·51	12·9	14·5	72·6
35	1·058	1·90	14·6	17·2	68·2	1·081	2·36	15·1	13·7	71·2	1·026	1·71	13·9	14·7	71·4
40	1·108	2·08	14·8	17·5	67·7	1·144	2·51	15·6	13·8	70·6	1·082	1·89	15·0	14·8	70·2
45	1·148	2·23	15·1	17·5	67·4	1·183	2·65	16·1	13·8	70·1	1·123	2·04	15·5	14·9	69·6
50	1·179	2·39	15·3	17·5	67·2	1·218	2·77	16·4	13·9	69·7	1·156	2·15	15·9	15·1	69·0
55	1·204	2·51	15·6	17·6	66·8	1·247	2·86	16·6	14·0	69·4	1·185	2·27	16·2	15·3	68·5
60	1·227	2·61	15·9	17·6	66·5	1·272	2·96	16·9	14·1	68·0	1·207	2·37	16·6	15·4	68·0
65	1·241	2·71	16·0	17·7	66·3	1·286	3·02	17·1	13·2	68·7	1·223	2·44	16·9	15·5	67·6
70	1·256	2·80	16·2	17·8	66·0	1·300	3·07	17·2	14·3	68·5	1·234	2·55	17·0	15·7	67·3
	$n = 33$;	$\alpha = 1{\cdot}15$;		$l = 17{\cdot}8$ mb		$n = 18$;	$\alpha = 1{\cdot}97$;		$l = 6{\cdot}5$ mb		$n = 46$;	$\alpha = 1{\cdot}95$;		$l = 10{\cdot}6$ mb	

Table 2. Spectral composition of direct solar radiation in mountain areas (after Lopukhin, 1957)

λ	Type I			Type II				Type III				Type IV			
	S (cal/cm²/min)	% of total radiation for λ (nm)		S (cal/cm²/min)	% of total radiation for λ (nm)			S (cal/cm²/min)	% of total radiation for λ (nm)			S (cal/cm²/min)	% of total radiation for λ (nm)		
		290–520	520–600		290–380	380–410	> 550		290–380	380–410	> 550		290–520	520–620	>625
2	0·25	7·7	13·9	0·430	2·10	6·4	85·7	–	1·36	4·6	84·2	–	–	–	–
5	0·66	8·9	13·8	0·640	2·30	6·8	84·9	–	1·58	4·8	83·4	0·41	10·3	11·5	78·2
10	1·02	11·2	13·7	0·930	2·60	7·3	83·1	0·736	1·82	5·2	82·0	0·63	11·4	12·0	76·6
15	1·20	13·3	13·5	1·075	–	7·7	82·0	0·935	–	5·5	80·8	0·78	12·2	12·4	75·4
20	1·30	14·9	13·3	1·175	2·96	8·1	80·7	1·080	2·17	5·7	79·9	0·92	13·0	12·6	74·4
25	1·38	16·2	13·2	1·244	–	8·4	79·9	1·175	–	6·1	78·8	–	–	–	–
30	1·42	17·2	13·2	1·246	3·17	8·7	79·2	1·220	2·47	6·3	78·0	1·11	14·6	12·8	72·6
35	1·46	18·1	13·1	1·325	–	9·0	78·6	1·250	–	6·5	77·2	–	–	–	–
40	1·49	18·9	13·1	1·350	3·34	9·3	78·1	1·263	2·58	6·6	76·4	1·21	17·1	13·5	69·4
45	1·52	19·5	13·1	1·357	–	9·6	77·7	1·280	–	6·7	76·0	–	–	–	–
50	1·54	20·1	13·1	1·380	3·62	9·7	77·3	1·306	2·70	6·8	75·6	1·27	19·6	13·9	60·5
55	1·56	20·4	13·0	1·400	–	9·9	76·9	1·320	–	6·9	75·3	–	–	–	–
60	1·57	20·7	13·0	1·420	3·88	10·2	76·6	1·330	2·78	7·0	75·0	1·35	21·2	14·3	64·5
65	1·58	21·0	13·0	1·422	4·00	10·3	76·3	1·336	–	7·0	74·8	–	–	–	–
70	1·59	21·3	13·0	1·424	4·10	10·5	76·0	1·340	2·80	7·1	74·7	1·37	–	–	–

Table 2. (*contd.*)

λ	Type V				Type VI				Type VII			
	S (cal/cm^2/min)	% of total radiation for λ (nm)			S (cal/cm^2/min)	% of total radiation for λ (nm)			S (cal/cm^2/min)	% of total radiation for (nm)		
		290–520	520–625	> 625		290–380	380–410	> 550		290–520	520–620	> 625
2	—	—	—	—	—	1·92	3·6	82·5	—	—	—	—
5	0·38	18·0	13·7	68·3	—	2·22	3·8	83·9	0·68	7·4	19·0	73·6
10	0·57	18·6	13·3	68·1	0·482	2·56	4·2	80·8	0·93	9·4	16·9	73·5
15	0·72	19·1	13·0	67·9	0·693	—	4·8	79·8	1·04	11·3	16·3	73·4
20	0·80	19·6	12·8	67·6	0·835	3·02	5·3	78·8	1·13	12·7	15·8	71·5
25	—	—	—	—	0·944	—	5·7	77·9	—	13·8	15·7	70·5
30	0·98	20·6	12·1	67·3	1·046	3·42	6·3	77·0	1·25	14·9	15·6	69·5
35	—	—	—	—	1·130	—	6·7	76·1	—	15·6	15·6	68·8
40	1·12	21·4	11·7	66·9	1·176	3·73	7·1	75·6	1·33	16·3	15·5	68·2
45	—	—	—	—	1·216	—	7·4	75·1	—	16·9	15·5	67·6
50	1·23	22·2	11·2	66·6	1·242	4·03	7·8	74·7	1·38	17·5	15·4	67·1
55	—	—	—	—	1·260	—	8·2	74·4	—	18·0	15·3	66·7
60	1·32	22·8	11·1	66·2	1·270	4·33	8·4	74·2	1·42	18·5	15·2	66·3
65	—	—	—	—	1·278	—	8·6	74·0	—	18·8	15·1	66·1
70	1·39	23·2	10·8	66·0	1·281	4·52	8·7	73·8	1·45	19·1	15·0	65·9

Note: For Type I, the number of cases $n = 10$, $\alpha = 0{\cdot}52$, $l = 5{\cdot}0$ mb; for Type II, $\alpha = 0{\cdot}82$, $l = 9{\cdot}6$; for Type III, $n = 5$, $\alpha = 1{\cdot}23$, $l = 9{\cdot}20$; for Type IV, $\alpha = 1{\cdot}4$; for Type V, $n = 10$, $\alpha = 1{\cdot}77$; for Type VI, $n = 7$, $\alpha = 1{\cdot}72$, $l = 10{\cdot}0$; for Type VII, $\alpha = 2{\cdot}0$.

Filter radiometry is now well suited for repetitive measurements of a particular source and is readily adapted to widely varied field conditions. Rather complete details of one such system have been given[6].

The primary objective of one phase of a NASA Office of Advanced Research and Technology sponsored program, "to have in hand a well-calibrated, well-understood multichannel radiometer which has been exposed to the extraterrestrial solar flux", has been accomplished and the principal results presented[7–9]. The results of some of the tests which were necessary to understand the performance of the radiometer system are discussed below. Since the basic sensitivity calibration effort was made at an elevation of 2·3 km (Table Mountain, California) and since it was necessary to coordinate these calibrations with the 80-km primary measurements, evaluation of radiometer performance at other altitudes and in different environments was accomplished. It has been possible during the last three years to fly the radiometric equipment thirty-six times at altitudes of about 12 km and greater, and to perform at least ten ground-based intercomparisons and basic calibrations; as a by-product of the fundamental study, data from these tests will provide measures of the atmospheric spectral attenuation.

INSTRUMENTATION

These multichannel radiometers, incorporating lens amplification in the narrow bandpass channels and using wirewound-plated thermopiles blackened to eliminate spectral selectivity, have been described by Drummond *et al.*[6]. The versatility of this radiometric system for field application is shown in Fig. 2 which is a photograph of the field station operating from the court house and jail at Parhump, Nevada. Figure 3 is a view of the radiometer mounted in its gimbal box during the NASA Ames Convair CV-990 1968 Solar Transit flights. The open gimbal mount was necessary in order to dispense with a window, the presence of which would have resulted in undesirable multiple reflection effects as well as limiting the source spectrum wavelengthwise. When the aircraft protective hatch was opened, the radiometer was directly exposed to the outside environment of −45°C and 550 m.p.h. wind velocity. Fortunately, the aircraft boundary layer greatly attenuated the severity of the radiometer environment. Careful testing failed to reveal any excess noise or other abnormalities in operation during flight exposure.

The adaptability of this type of multichannel radiometer can best be illustrated by the fact that, with relatively simple modification of mounting, it has been possible to install and operate the equipment at field stations at Table Mountain, at the NASA Lewis Laboratory hangar apron (Cleveland, Ohio), aboard the NASA Lewis B-57B jet aircraft and the NASA Edwards X-15 rocket aircraft, and both inside and in the external gimbal box of the NASA Ames CV-990 jet. Readout equipment appropriate to the operational conditions has been used. This ranges from conventional microvolt-type amplifiers, coupled to stripchart millivolt recorders or integrating digital voltmeters and printers, to the specially developed commutator/amplifier for the X-15 flights.

CALIBRATION

Because the multichannel radiometers were to be used for fundamental extraterrestrial measurements, extreme care was observed during the series of basic calibration efforts. All radiometers were referred to a group of Eppley–Ångström, working-

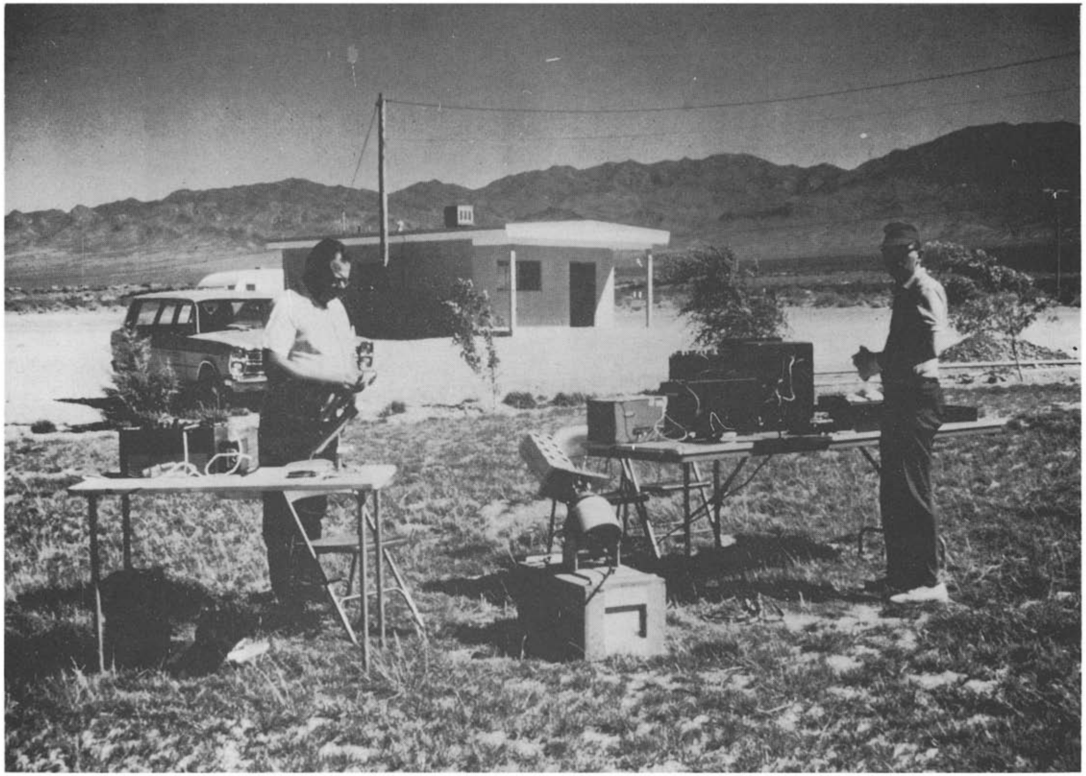

Fig. 2. SSME field station, Parhump, Nevada, 1967.

[Facing page 50]

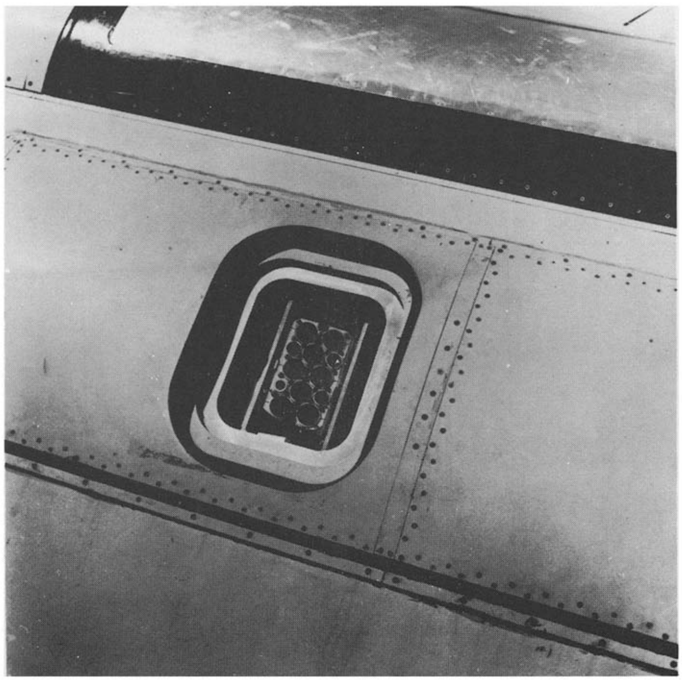

Fig. 3. Multichannel radiometer as installed in the CV-990 gimbal mount, outside view (photograph courtesy, NASA Ames).

Fig. 4. Table Mountain calibration set-up.

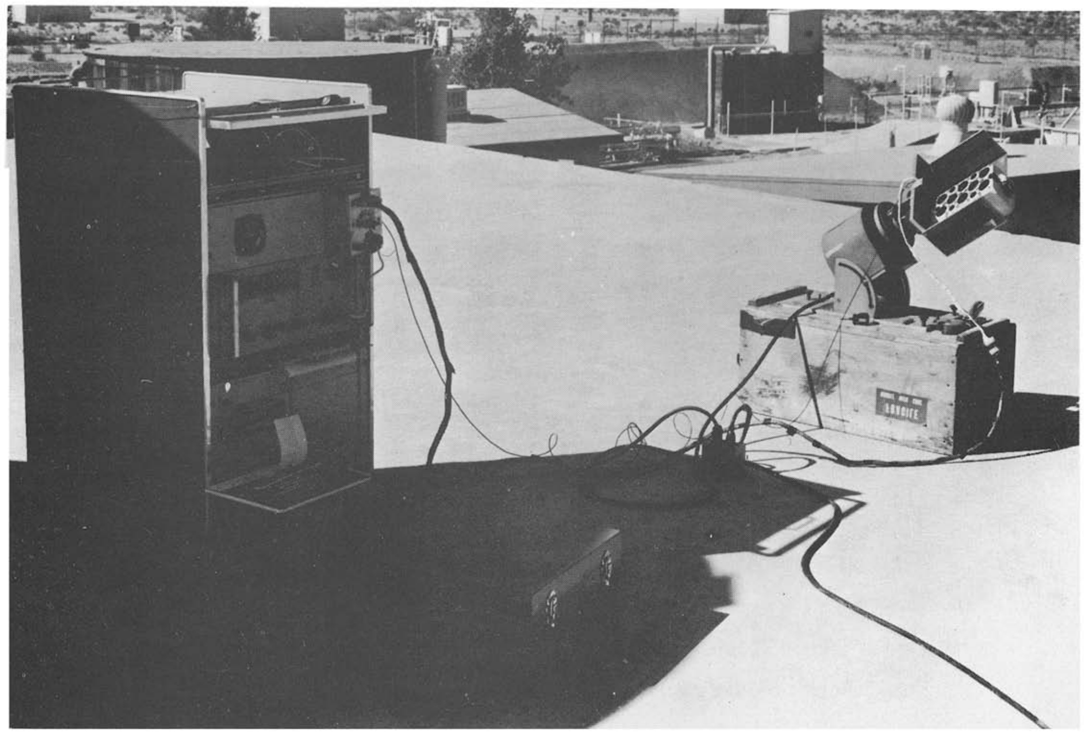

Fig. 5. JPL Edwards Test Station site.

standard, electrical-compensation pyrheliometers. In turn, these pyrheliometric standards were frequently compared with the U.S. national pyrheliometric standards maintained at Newport, R.I., to reproduce the IPS fundamental reference. Calibration of the broad-band and total channels was achieved at Table Mountain (Fig. 4) and at 12 km aboard the CV-990 aircraft. Agreement between these latter calibrations was within 1 per cent on all four channels. Three multichannel radiometers have been used for this program. The two operational instruments are exposed to environmental extremes, while the third is carefully protected and employed mainly for rapid intercomparison with the operational units before and after each flight. Establishing the basic sensitivity of the narrow-band, lens-type detectors is a more difficult procedure. Because the lenses effectively amplify the irradiance at the thermopiles, it is not possible to expose the lens/thermopile arrangement directly to the Sun. A series of neutral density attenuators (attenuation factors of approximately 0·1, 0·05, 0·033, 0·025 and 0·02) is calibrated at the field site using a large, high-sensitivity thermopile or a cavity detector. Knowing the local solar irradiance (Ångström measurements) and the signal from the lens/thermopile when irradiated through the attenuators, it is possible to compute the sensitivities of the narrow wavelength channels.

So that valid data can be acquired even though the radiometer is not precisely aligned with the Sun, it is necessary that the solar image through the lens irradiates more than just the area of the thermopile. Operation in this defocused condition requires correction for any significant chromatic aberration in certain spectral regions.

Confidence in the validity of the various channel sensitivities, filter factors and aberration corrections has been acquired after many repetitive measurements. A minimum of 10 individual measurements per session, involving numerous separate calibration efforts, are made and examined for spread and consistency with other data before a value is accepted for use. In this way, the state-of-the-art in the transfer from a radiometric standard to an instrument field operation has been advanced.

EXPERIMENTAL DATA

Because the major effort was to calibrate the radiometers, all of the data were obtained under as nearly ideal, clear-sky conditions as possible. The temporal stability of the total solar irradiance at Table Mountain on good observing days has been found to vary less than 0·5 per cent during the 30 min before and after the local solar noon. In such calibration programs, it is necessary to examine the atmospheric effects determining the variance of radiant flux.

The particular experiment to be described involved inter-comparing two multichannel radiometers at Table Mountain (TM) at 2·3 km elevation, and then transporting one of the radiometers to the JPL Edwards Test Station site (ETS), 60 mi north and at 1·3 km elevation (Fig. 5). To illustrate the spectral attenuation effects, concurrent observations at the two sites (within what was predicted to be the same weather system) were made throughout the succeeding day.

The comparative values of the total irradiance throughout one day at both test sites are shown in Fig. 6 (see also Fig. 10). Here, the solar intensities have been plotted against the local *absolute* optical air mass (m) values (where $m =$ sec solar zenith angle $\times\, p/p_0$, p being the atmospheric pressure at the location and p_0 the mean sea level pressure—usually taken to be 760 Torr). The asymmetrical nature of these curves is

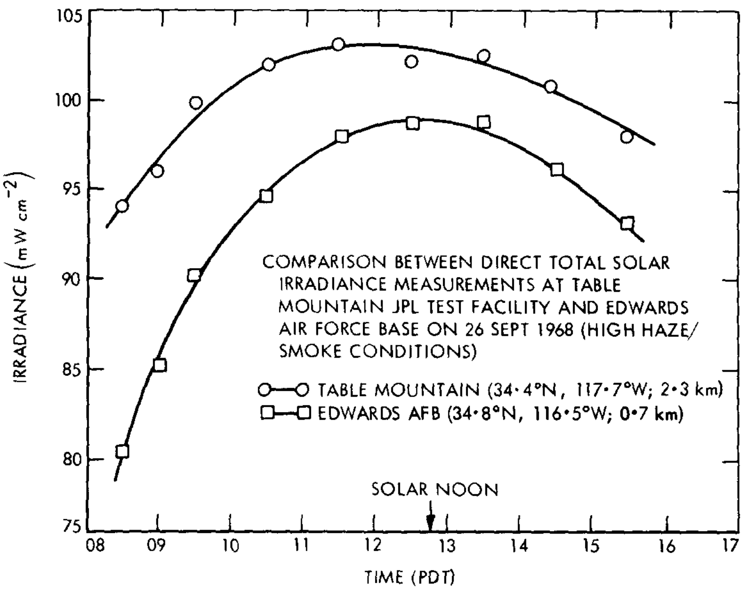

Fig. 6. Total irradiance intercomparison; Table Mountain (TM) and Edwards Test Station (ETS).

believed to be caused by high-level aerosol associated with the Santana weather condition.

The associated Figs. 7–9 give this temporal kind of information, respectively, for the spectral regions (1) λ 290–344 nm (i.e. the lower half of the ultraviolet to which the atmosphere is transparent), (2) λ 507–589 nm (i.e. the yellow–orange portion of the

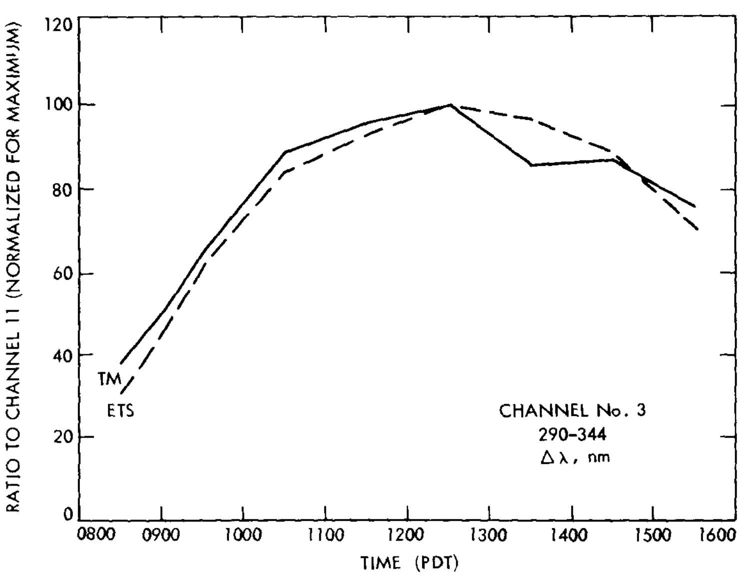

Fig. 7. Spectral irradiance, 290–344 nm; proportion of total flux.

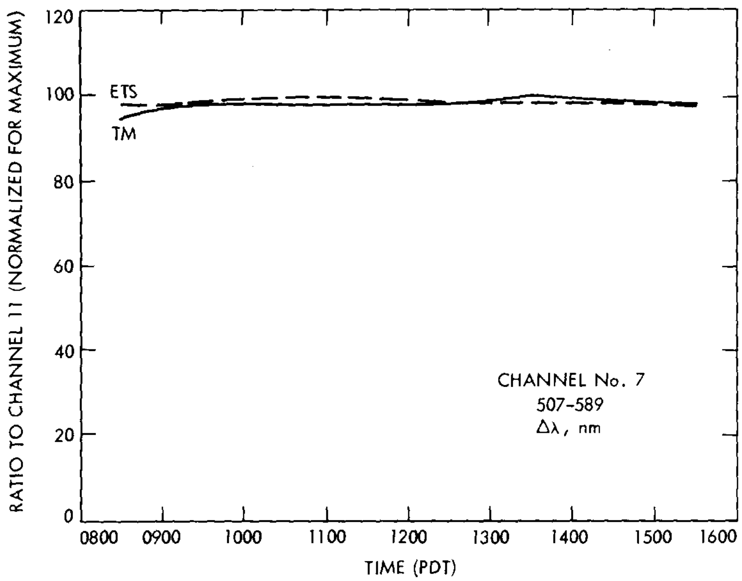

Fig. 8. Spectral irradiance, 507–589 nm; proportion of total flux.

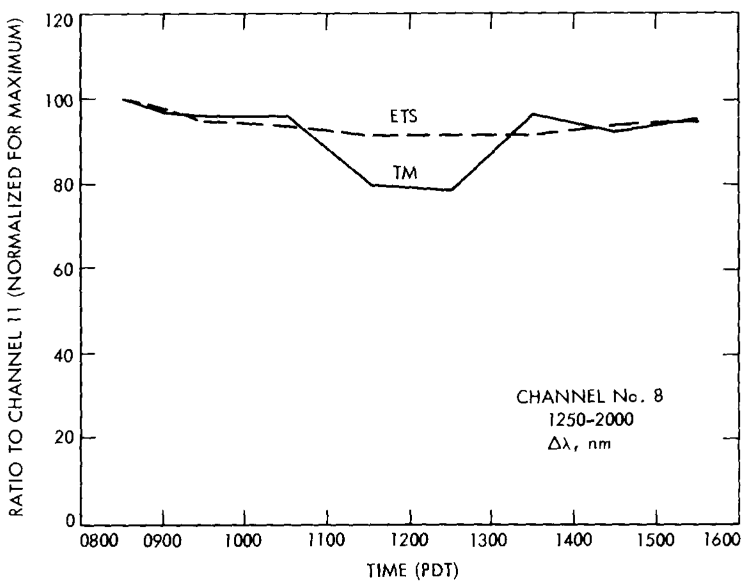

Fig. 9. Spectral irradiance, 1250–2000 nm; proportion of total flux.

visible), and (3) λ 1250–2000 nm (i.e. part of the near infrared). In all cases, these pairs of curves have been expressed in relative manner, as ratios of the signals from the particular narrow-bandpass filter channels to the total flux. Figures 11–13 are somewhat complementary in providing an insight to the spectral attenuation at the two locations. Here, the measurements plotted (in absolute values) refer to the simul-

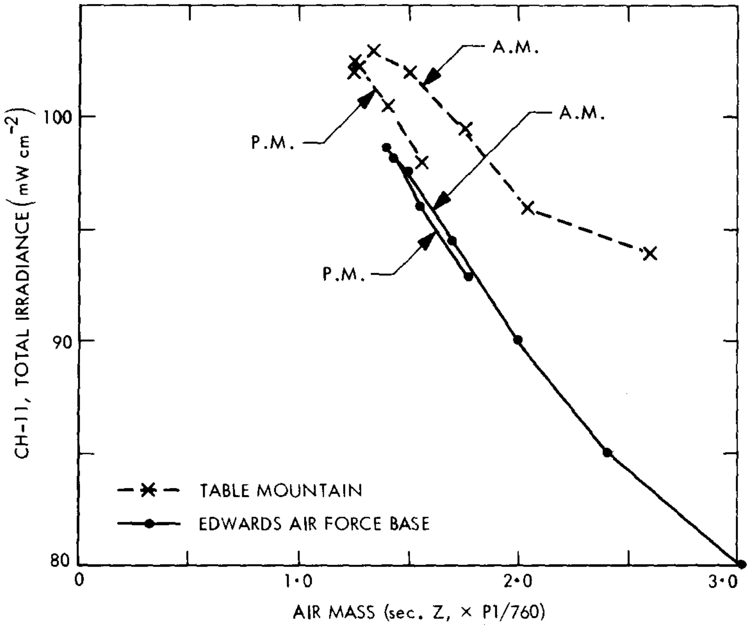

Fig. 10. Concurrent TM/ETS; total irradiance vs. air mass.

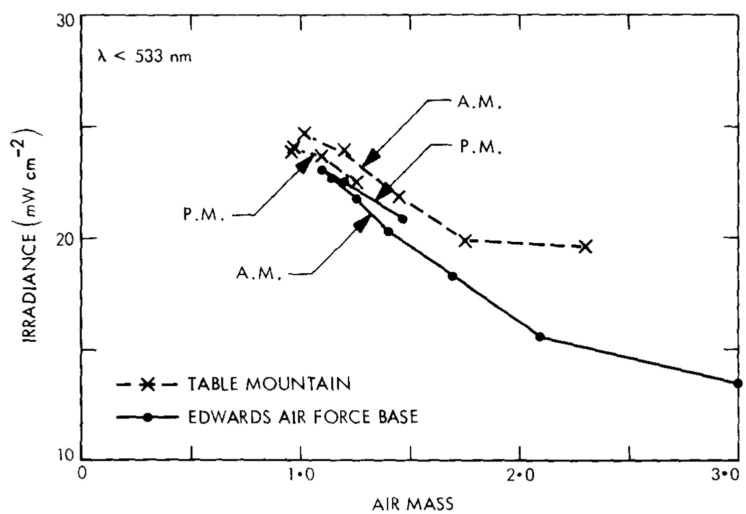

Fig. 11. Concurrent TM/ETS; $\lambda < 533$ nm irradiance vs. air mass.

taneously observed broad-bandpass filter channels, viz. (1) $\lambda < 533$ nm (i.e. total flux − OG1 filter; ultraviolet + lower visible), (2) $\lambda > 533$ nm (OG1 filter; upper visible + near infrared), and (3) $\lambda > 697$ nm (RG8 filter; near infrared).

If only the geometrical aspect of the air mass parameter was involved, such a normalization procedure as adopted for the above-mentioned presentations would simply represent an instrumental check on radiometer performance. But there is also

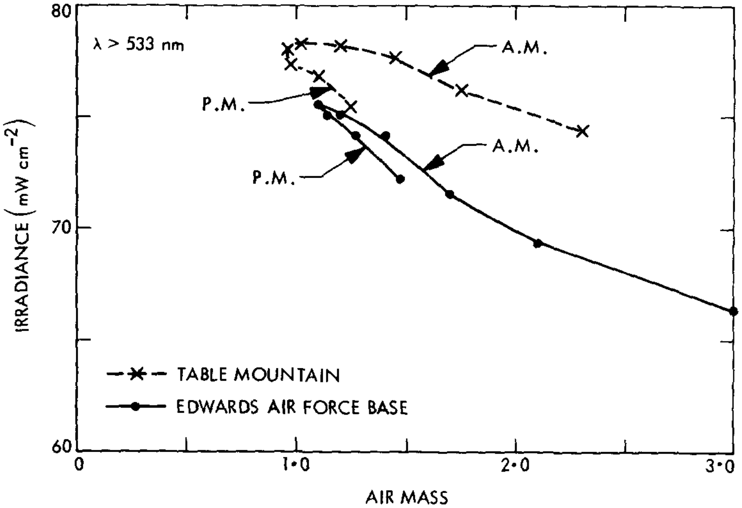

Fig. 12. Concurrent TM/ETS; λ > 533 nm irradiance vs. air mass.

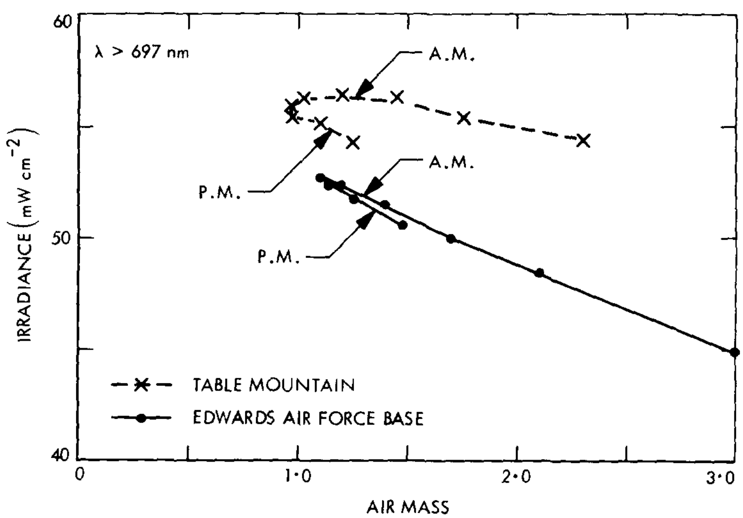

Fig. 13. Concurrent TM/ETS; λ > 697 nm irradiance vs. air mass.

the meteorological aspect which is manifest through atmospheric extinction along the particular (local) solar path. This effect is a result of the scattering by molecules and by solid and liquid particulate matter (aerosol), and of the selective absorption mainly by water vapor, carbon dioxide and ozone. Inspection of the narrow-band curves reveals the different influences of the atmospheric pollutants and the water-vapor vertical profiles at the locations. Despite their relative close proximity (approximately 100 km), there are marked divergences, at times, between some of the corresponding pairs of curves. Clearly, the altitude difference (1·6 km) effect on this day is secondary to those effects caused by the local air structures above each of the observation sites. Whereas the shorter solar wavelengths (e.g. $\lambda < 533$ nm) are significantly depleted by energy diffused out of the beam of sunlight by aerosol, the near infrared contribution (in this instance, $\lambda > 697$ nm) is markedly subject to the prevailing concentration of water vapor. For example, the latter condition is strikingly demonstrated by the apparent temporary increase in the moisture content above Table Mountain around noon (producing the decrease in the irradiance in the infrared region), which was not the case at the Edwards (Air Force Base) Test Site (see Fig. 9). On the other hand, the influence of dust and smoke (smog) over Table Mountain in the mid afternoon, on the ultraviolet record, is evident (see Fig. 7). As would be expected, the upper visible component at both sites was scarcely affected since this is a wavelength interval where atmospheric scattering and absorption effects are minimum.

The fact that such useful information can be gained from spectral measurements of the direct solar radiation, even in relatively broad filtered bands as well as in more selective narrow bands, is indicative of the need to amplify the more customary (i.e. integral wavelength) flux measurements by subdivision of the energy spectrum. There is no question of the importance of such filter techniques as tools, not only in geophysical and astrophysical research, but also in increasing our knowledge of local weather and climate at the Earth's surface.

During many of the calibration sessions at Table Mountain, it has been observed that a temporal instability (i.e. the irradiance vs. time, on a strip-chart recorder, of the 300–350 nm band would randomly vary 10–15 per cent in a period of 2 min) would be apparent 45 min before any appreciable (1–2 per cent) instability of the total irradiance was noted. This variation in stability of the 300–350 nm band appears to be a sensitive precursor to the normal deterioration in solar irradiance. It is believed that this variability has not been properly studied, and it is suggested that here is a possible index for meteorological interpretation.

CONCLUSIONS

The most salient observation one can make in the field of solar spectral irradiance is the difficulty of coordinating the various observations because of the wide variety of pass bands used for the measurements. Since the primary purpose of the work reported upon was the establishment of the solar constant and its spectral components, the local climatological aspects have only been treated in a very preliminary manner.

As explained, the filter radiometer has the advantage of simplicity, reliability and relative ease of data acquisition and interpretation. The application of this type of instrumentation to meteorology represents a logical step in the process of increasing the understanding of our environment. Initial efforts to define the relationship between the observed ultraviolet instability and atmospheric conditions may prove highly valuable. Measurement of the spectral irradiance in the 1200–2000 nm region may well prove to be a valuable indicator of the atmospheric moisture content. The work of Lopukhin[3] deserves more careful study with regard to the classification of atmospheric attenuation.

The first step might be to make routine measurements of the solar ultraviolet and the infrared in well-defined spectral regions, as a function of the integral wavelength irradiance.

REFERENCES

[1] R. K. Kunkel, P. A. C. Cook, A. J. Drummond and W. J. Scholes, Precision spectral measurements of direct solar radiation: an analysis of extended daily values for Arizona and Florida. Paper presented at the *Fourth Annual Meeting of the Solar Energy Society*, Palo Alto, 1968 (to be published).
[2] P. Moon, Proposed standard solar-radiation curves for engineering work. *J. Franklin Inst.* **230**, 583 (1940).
[3] E. A. Lopukhin, Spectral composition of direct solar radiation. *Geliotekhnika* **1**, 44 (1957); translation available, N6632857, from Supt. Documents, U.S. Government Printing Office, Washington, D.C., 20402.
[4] J. S. Nader, *Pilot study of ultraviolet radiation in the Los Angeles basin, October 1965*. U.S. Public Health Publication, Washington, D.C., No. 999-AD-38 (1967).
[5] J. C. Arvesen, R. N. Griffin, Jr. and D. D. Pearson, Jr., Determination of extraterrestrial solar spectral irradiance from a research aircraft. *J. App. Optics* **8**, November issue (1969).
[6] A. J. Drummond, J. R. Hickey, W. J. Scholes and E. G. Laue, Multichannel radiometer measurement of solar irradiance. *J. Spacecraft and Rockets* **4**, 1200 (1967).
[7] A. J. Drummond, J. R. Hickey, W. J. Scholes and E. G. Laue, New value for the solar constant of radiation. *Nature* **218**, 259 (1968).
[8] E. G. Laue and A. J. Drummond, Solar constant: first direct measurements. *Science* **161**, 888 (1968).
[9] A. J. Drummond and J. R. Hickey, The Eppley-JPL solar constant measurement program. *Solar Energy* **12**, 217 (1968).